MECSOL 2019 - Proceedings of the 7th International Symposium on Solid Mechanics,
V. Tita, A. Ferreira, M.L. Ribeiro, A. Vieira and A.T. Beck (Editors), ABCM, Sao Carlos, SP, Brazil, April 15th to 17th, 2019

Residual stress distribution in hyperstatic beams

Flávio Assumpção de Castro [1], Paulo Pedro Kenedi [1], Lucas Lisboa Vignoli [2,3] and Ivan Ivanovitsch Thesi Riagusoff [4]

[1] Programa de Pós-Graduação em Engenharia Mecânica e Tecnologia de Materiais (PPEMM) – CEFET/RJ, Brazil

[2] Mechanical Engineering, Universidade Federal do Rio de Janeiro – Campus Macaé, Brazil

[3] Center of Nonlinear Mechanics, COPPE, Mechanical Engineering Department, Universidade Federal do Rio de Janeiro, Brazil

[4] Rosenbra Engenharia Brasil Ltda, Brazil

Abstract: The estimative of the cross section residual stress distribution, for partially yielded structures, is an important subject that should be addressed to guarantee the stress analysis modeling correctness. In fact, the lack of the knowledge of residual stress distribution in partially yielded cross sections can possibly lead to an unsafe equipment design. The residual stress distributions for static beams (but not hyperstatic beams) have been extensively studied, using mechanics of solids, habitually for simple cases. Expanding this approach, this work analyses the residual stress distribution, for critical cross sections, of hyperstatic beams. The analytical model is presented, in a detailed way, with the residual stress distribution of a fixed end beam critical cross sections being explicitly plotted. One of the main conclusions of this work is that important levels of residual stresses can grow up, away from external surfaces, where most of the experimental residual stress measurements may not have access, creating a potentially unsafe situation.

Keywords: residual stress, hyperstatic structures, analytical model

INTRODUCTION

The residual stress distribution, in partially yielded cross sections of structures, can occur as result, for instance, of an overload event. Although residual stresses can reach high values, if compared to the yield resistance of the material, in most cases they are not often taken in consideration. The lack of knowledge in various areas as: plastic hinge formation and the residual stress cross section distribution; can contribute to this situation. Nevertheless, Castro and Meggiolaro (2009) present an analytical approach of the residual stress distribution of partially yielded static structures that is very instructive. Also, Lopes (2013) did an interesting analytical/experimental work about the residual stress distribution in partially yielded tensile armour wires, for different impose curvature radius. Other authors focuses on plastic hinge critical loads as Amdahl (2005), that presented examples of application of the unit load method to solve hyperstatic structures, estimating the sequence of plastic hinge critical loads. Also, Caprini (2007) show an introductory text about plastic analysis of structural engineering, including the obtention of hyperstatic beams plastic hinge critical loads. Jiásek and Bazant (2002) presents an interesting chapter about the use of matrix structural analysis to describe the evolution of the structure forces, bending moments, displacements and slopes for determinate points (nodes) during sequential plastic hinge formation.

In this work a fixed end beam, with a concentrated load P is studied. As the beam has two degree of indetermination, three plastic hinge generation were expected as P value grows. The proposed analytical model uses an incremental approach to access the bending moment distribution, the plastic hinge critical loads and thus the residual stresses distribution, as can be shown in the next section, Castro (2018).

ANALYTICAL MODEL

An incremental approach is used in the proposed analytical model. The model is based on the estimation of the beam longitudinal bending moment, at every beam section, for each of the crescent load values. Besides the obtention of the final critical load, which forms the last plastic hinge that fails the structure, also the intermediary critical loads (of intermediary plastic hinges) are accessed. The material is supposed to behave as elastic perfectly plastic and the beam

has a rectangular cross section. A fixed end beam with a transversal concentrated load was used exemplify the model application.

Fig. 1 shows a free body diagram of a fixed end beam (fixed at sections *A* and *B*), with a decentralized vertical concentrated load P_0, applied at section *C*, and also the rectangular cross section partially yielded:

(a) (b)

Figure 1 – Fixed end beam: (a) free body diagram and (b) partial yielded cross section.

Where *b* and *c* are, respectively, the cross-section width and semi-height; y_y is the height of the elasto-plastic border. For the elastic situation of Fig. 1.a, the reactions can be calculated, using the method of superposition, with equilibrium equations and the additional aid of slope and deflection equations, as in Crandall *et. al*. (1978):

$$R_{A0} = \frac{(L-a)^2(L+2a)}{L^3}P_0 \qquad R_{B0} = \frac{a^2(3L-2a)}{L^3}P_0 \qquad M_{A0} = \frac{a(L-a)^2}{L^2}P_0 \qquad M_{B0} = \frac{a^2(L-a)}{L^2}P_0 \tag{1}$$

Where, R_{A0}, R_{B0}, M_{A0} and M_{B0} are reactions, *L* is the beam length, *a* is the concentrated load position (in relation to section A end).

A rectangular cross section, as shown in Fig.1.b, begins to yield when the beam is submitted to a bending moment that reach M_y (when y_y = c), which expression is shown at equation (2.a). When the cross section is completely yielded, the beam is submitted to the plastic bending moment M_P (when y_y = 0), which value is shown at equation (2.b).

$$M_Y = \frac{2}{3}bc^2S_y \qquad M_P = bc^2S_y \tag{2}$$

Dividing equation (2.b) by equation (2.a) it is possible to estimate the shape factor, for a rectangular cross section, α =1.5. At the next section the beam moment distribution is calculated for every critical load.

Fixed end beam bending moment distribution

As the concentrated load *P* keep increasing its value, three beam cross sections reach, in sequence, the complete cross section yield (plastic hinge), leading the beam to a total failure as *P* reaches the third critical load. Fig. 2 shows, in a schematic way, the beam configurations used to estimate the beam reactions, the critical loads and bending moment distribution for the various loading levels, Castro (2018).

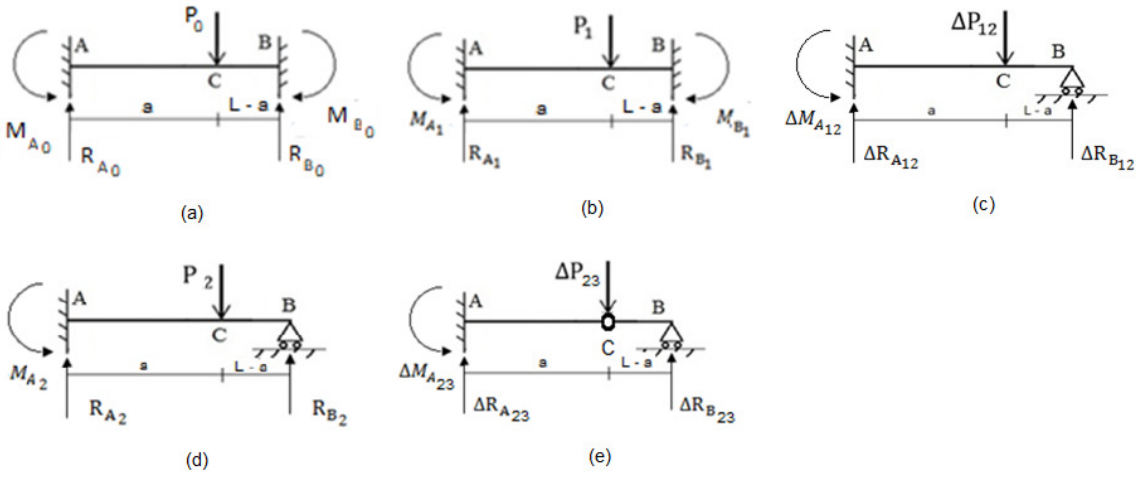

Figure 2 – Fixed end beam loading incremental phases: (a) before the first critical load, (b) at first critical load, (c) the load increment between first and second critical loads, (d) at second critical load and (e) the load increment between second and third critical loads.

Note that the load increment between first and second critical loads ΔP_{12} changes to ΔP_2 when P reaches P_2. In the same way the load increment between second and third critical loads ΔP_{23} changes to ΔP_3 when P reaches P_3. For the first critical load P_1 the reactions are considered being the same of (1) just replacing P_0 by P_1:

$$R_{A1} = \frac{(L-a)^2(L+2a)}{L^3}P_1 \qquad R_{B1} = \frac{a^2(3L-2a)}{L^3}P_1 \qquad M_{A1} = \frac{a(L-a)^2}{L^2}P_1 \qquad M_{B1} = \frac{a^2(L-a)}{L^2}P_1 \tag{3}$$

The bending moment distribution for the first critical load P_1 is described by:

$$M_1(x) = -M_{A1} + R_{A1}x \quad \text{for } 0 \le x \le a \qquad M_1(x) = -M_{B1} + R_{B1}(L-x) \quad \text{for } a < x \le L \tag{4}$$

Fig. 3.a shows the bending moment distribution at the critical load P_1. The bending moment distribution for the second critical load P_2 is described by:

$$\Delta M_2(x) = -\Delta M_{A2} + \Delta R_{A2}x \quad \text{for } 0 \le x \le a \qquad \Delta M_2(x) = -\Delta M_{A2} + \Delta R_{A2}x - \Delta P_2(x-a) \quad \text{for } a < x \le L \tag{5}$$

$$M_2(x) = M_1(x) + \Delta M_2(x) \tag{6}$$

$$\text{where, } \Delta R_{A2} = \frac{2L^3 - 3aL^2 + a^3}{2L^3}\Delta P_2 \qquad \Delta M_{A2} = \frac{a(2L^2 - 3aL + a^2)}{2L^2}\Delta P_2 \qquad \Delta P_2 = \frac{(2a-L)2L^2}{a^2(L-a)(3L-a)}M_P \tag{7}$$

The bending moment distribution for the third critical load P_3 is described by:

$$\Delta M_3(x) = -\Delta M_{A3} + \Delta R_{A3}x \quad \text{for } 0 \le x \le a \qquad \Delta M_3(x) = -\Delta M_{A3} + \Delta R_{A3}x - \Delta P_3(x-a) \quad \text{for } a < x \le L \tag{8}$$

$$M_3(x) = M_1(x) + \Delta M_2(x) + \Delta M_3(x) \tag{9}$$

$$\text{where, } \Delta R_{A3} = \Delta P_3 \qquad \Delta M_{A3} = a\Delta P_3 \qquad \Delta P_3 = -\frac{L(L-2a)}{a^2(3L-a)}M_P \tag{10}$$

Note that it is quite clear the sequence of cross sections yielding through the observation of the bending moment levels at each cross section in Fig. 3: first at section *B* (right end), then at section *C* (at *P* section) and finally at section *A* (left end).

RESULTS

Using the development of the analytical model, Castro (2018), it is possible to obtain the values of the plastic hinge critical loads, bending moment beam distribution and cross section residual stress distribution.

Fixed end beam critical loads

For the fixed end beam with a transversal concentrated load positioned at a from A end, the first critical load P_1 can be easily estimated by imposing M_p to the moment reaction M_{B1} show at equation (3.d):

$$P_1 = \frac{L^2}{a^2(L-a)}M_p \tag{11}$$

To access the second critical load P_2 it is only necessary to use equations (7.c) and (11) in (12.a):

$$P_2 = P_1 + \Delta P_2 \qquad P_2 = \frac{L^2(L+3a)}{a^2(L-a)(3L-a)}M_p \tag{12}$$

To access the third, and last, critical load P_3, it is only necessary to use equations (10.c) and (12.b) in (13.a):

$$P_3 = P_2 + \Delta P_3 \qquad P_3 = \frac{2L}{a(L-a)} M_p \tag{13}$$

Dividing equation (13.b) by equation (11) it is possible to estimate the capacity of this hyperstatic structure to support additional 0.33· P_1 load after first plastic hinge generation.

Fixed end beam bending moment distribution graphics

The bending moment distribution for the fixed end beam for various loads can be accessed through the utilization of equations (3-10), which can be implemented graphically through the utilization of mathematical software, like Mathlab.

Fig. 3 shows the bending moment distribution M_i (x) for the three critical loads.

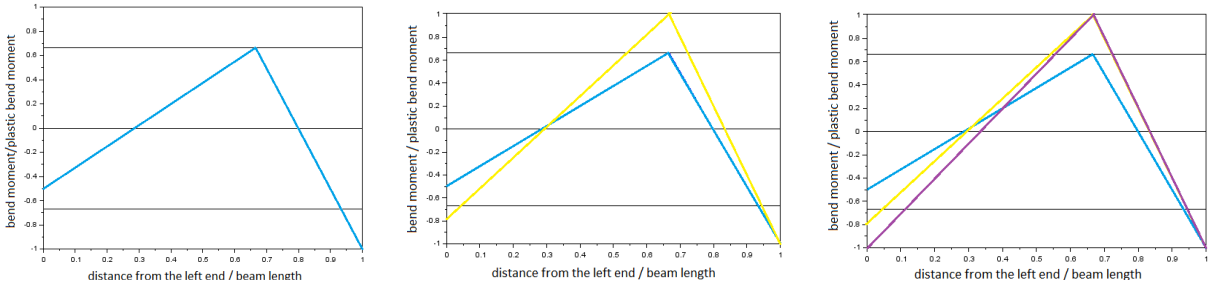

(a) (b) (c)

Figure 3 – Bending moment distribution evolution through beam length for critical load for: (a) P_1 (blue line), (b) P_2 (yellow line) and (c) P_3 (purple line).

Note that, in Fig. 3, at the x-axis the beam length was normalized by dividing x by L (beam length) and at the y-axis the bending moment was normalized by dividing M_i(x) by M_p (plastic moment). At first critical load, completely yields the B section generating M_1(x/L=1) / M_p = -1, partially yielding both A and C sections, as shown in Fig.3.a. At second critical load, completely yields the C section generating M_2(x/L=2/3) / M_p = +1, maintaining B section completely yielded and A section partially yielded. At third critical load at A section the M_3(x/L=0) / M_p = -1 value was reached, as shown in Fig.3.c, maintaining sections B and C also totally yielded. When this last critical load is reached, the fixed end beam completely fails.

Fixed end beam cross section residual stress distribution

To estimate the cross section residual stress distribution, as for instance, at sections A, B and C; it is necessary to obtain the bending moment distribution through the beam M_i (x), as done in equations (3-10). Using equation (14) is possible to estimate the residual stress distribution, at all the three plastic hinge cross sections.

$$\sigma_R(x,y) = \begin{cases} -S_y + \dfrac{M_i(x)y}{I} & for \quad y_y \le y \le c \\ -\dfrac{y}{y_y}S_y + \dfrac{M_i(x)y}{I} & for \quad -y_y \le y \le y_y \\ S_y + \dfrac{M_i(x)y}{I} & for \quad -c \le y \le -y_y \end{cases} \quad \text{where} \quad y_y = c\sqrt{3\left(1 - \frac{M_i(x)}{M_p}\right)} \qquad I = \frac{2}{3}bc^3 \tag{14}$$

Where, i is the critical load number and M_i(x) is the bending moment for cross sections: A (x/L = 0), B (x/L = 1) and C (x/L = 2/3). Note that equation (14.a) is formed by the sum of loading moment (with $M_y \le M_i(x) \le M_p$) and unloading moment (spring-back), up to $M_{sb} = 2 \cdot S_y$). Also, it is interesting to note that in every cross section are two distinct parts, as show in Fig.1.b, the elastic nucleus inside $-y_y \le y \le y_y$, and the yielded region outside this region.

Fig. 5 shows the graphical representation of equation (14). Note that the three cross section residual stress distribution were analysed all way to P_3 (but not including this last load) because after reaching it there is a completely fail of the structure.

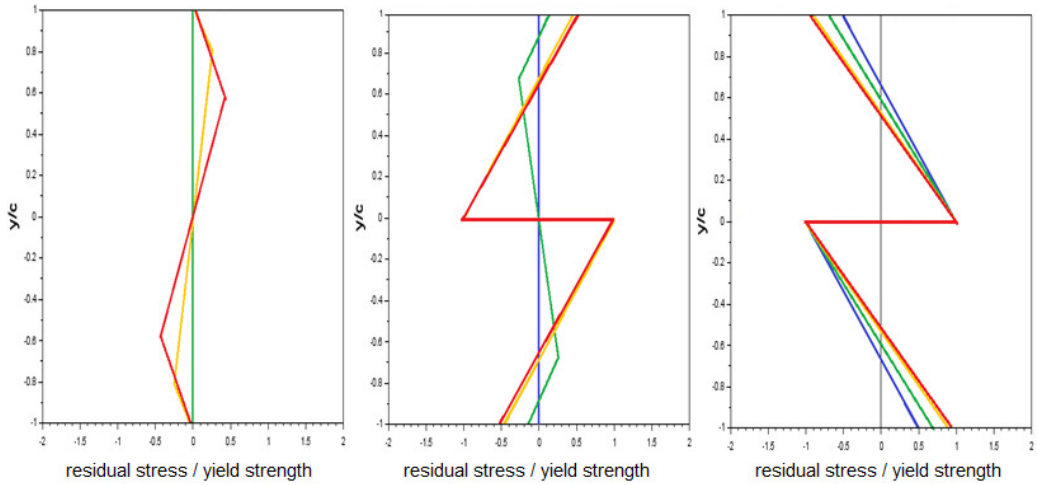

(a) (b) (c)

Figure 5 – Residual stress distribution for several loading phases for section: (a) A, (b) C and (c) B.

Analysing Fig. 5, where blue lines are related to P_1, the green lines are related to P_{12}, the yellow lines are related to P_2 and the red lines are related to P_{23}. Nevertheless, it is interesting to see that the three sections (*A*, *C* and *B*) have very distinct residual stress distribution. The section *B* was fully affected by the generation of the first plastic hinge, maintaining the cross section fully yielded up to the final failure. Section *A*, which was the last generating plastic hinge section, reveal a distinct behaviour, with a residual stress distribution with much lower values. The section *C* presented an intermediary behaviour between sections *A* and *B*. Finally note that in section *B* and *C* the highest residual stress values occur well inside the cross sections, far from external surfaces, where experimental methods usually are used.

CONCLUSIONS

In this research an analytical model was proposed, with the use of incremental approach, to follow the bending moment distribution through a fixed end beam, loaded with crescent values of *P*. All three critical loads, responsible for plastic hinge formation, were accessed, as well as, the residual stress distribution in the plastic hinge cross sections.

REFERENCES

Amdahl, J., 2005, "TMR4205 Buckling and Ultimate Strength of Marine Structures Chapter 1: Elastic-Plastic Analyses of Beams, Frames and Plates", http://www.ivt.ntnu.no/imt/courses/tmr4205/literature/chpt1_Elastic-plastic_analyses.pdf.

Crandall, S.H., Dahl, N.C. and Lardner, T.J., 1978, "An Introduction to the Mechanics of Solids", Second Edition with SI units, McGraw Hill International Editions.

Caprani, C., 2007, "Plastic Analysis – Structural Engineering", Faculty of Engineering, Monash University, Melbourne – Austrália, https://www.colincaprani.com/files/notes/SAIII/Plastic%20Analysis.pdf.

Castro, F.A., 2018, "Análise de tensões residuais em estruturas hiperestáticas" Master Thesis in portuguese, Centro Federal de Educação Tecnológica Celso Suckow da Fonseca - CEFET/RJ, Rio de Janeiro, Brazil.

Castro, J.T.P., Meggiolaro, M.A, 2009, "Fadiga – Técnicas e Práticas de Dimensionamento Estrutural sob Cargas Reais de Serviço. Volume 1- Iniciação de Trincas", Amazon.

Jirásek, M. and Bazant, Z.P., 2002, "Inelastic Analysis of Structures", John Wiley and Sons Ltd.

Lopes, D. G., 2013, "Avaliação das tensões residuais na montagem de conectores em armaduras de tração de dutos flexíveis", Master Thesis in portuguese, Centro Federal de Educação Tecnológica Celso Suckow da Fonseca - CEFET/RJ, Rio de Janeiro, Brazil.

RESPONSIBILITY NOTICE

The authors are the only responsible for the printed material included in this paper.

APPENDIX

Limit analysis approach:

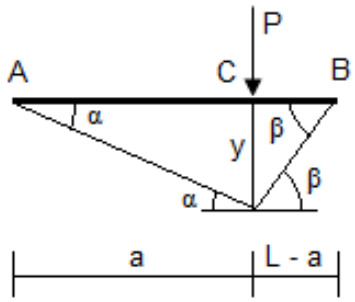

Figure A.1 – Limit analysis applied to a fixed end beam with a decentralized concentrated load.

From geometric manipulations is simple to see that:

$$\beta = \frac{a}{L-a}\alpha \tag{A.1}$$

Equating the internal and external virtual work:

$$P(\alpha a) = M_p\alpha + M_p(\alpha+\beta) + M_p\beta \tag{A.2}$$

After simple algebraic manipulations:

$$P = \frac{2L}{a(L-a)}M_p \tag{A.3}$$

Note that the equations (13) and (A.3) are the same.

Yielded regions:

Using equation (14.b), which relates the cross section elasto-plastic border $y_y(x)$ with the applied moment $M_i(x)$, it is possible to generate the lateral view of the elasto-plastic borders for horizontal (x/L) and vertical (y/c) positions.

$$\frac{y_y(x)}{c} = \sqrt{3\left(1-\frac{M_i(x)}{M_p}\right)} \qquad \text{(repeated)} \tag{14.b}$$

The yielded regions (marked in blue) at three different loading moments that corresponds to the critical loads: P_1, P_2 and P_3:

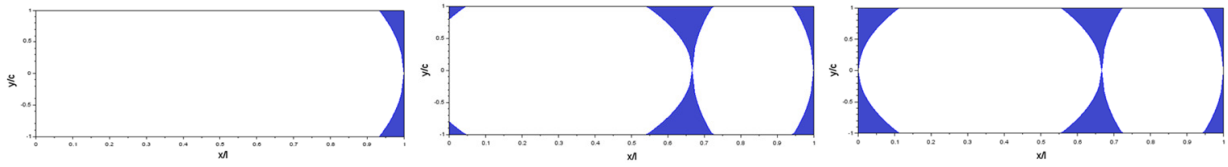

(a) (b) (c)

Figure A.2 – Yielded regions (beam lateral view) for the three critical loads are: (a) P_1, (b) P_2 and (c) P_3.

Note that, in Fig. A.2, at the x-axis the beam length was normalized by dividing *x* by *L* (beam length) and at the y-axis the beam height was normalized by dividing *y* by *c* (beam semi-height). The fixed end beam remains functional even with two sections completely yielded (plastic hinge) as in Fig.A.2.b. But, as soon as the *P* reach P_3 (collapse load) as shown in Fig, A.2.c, the fixed end beam completely fails.